IEEE Access
Multidisciplinary | Rapid Review | Open Access Journal

Received May 5, 2021, accepted May 11, 2021, date of publication May 17, 2021, date of current version May 24, 2021.

Digital Object Identifier 10.1109/ACCESS.2021.3081024

Complexity Analysis of Three-Dimensional Fractional-Order Chaotic System Based on Entropy Theory

GUOHUI LI, XIANGYU ZHANG, AND HONG YANG
School of Electronic Engineering, Xi'an University of Posts & Telecommunications, Xi'an 710121, China
Corresponding authors: Guohui Li (lghcd@163.com) and Hong Yang (uestcyhong@163.com)

This work was supported by the National Natural Science Foundation of China under Grant 51709228.

ABSTRACT Complexity analysis of fractional-order chaotic system is an interesting topic in recent years. How to measure the complexity of fractional-order chaotic system correctly and effectively is the basis of its theoretical analysis and engineering application. In this paper, complexity analysis of three-dimensional fractional-order chaotic system based on multivariate multiscale fuzzy entropy (mvMFE), multivariate multiscale sample entropy (mvMSE) and multivariate multiscale dispersion entropy (mvMDE) respectively is proposed. In the case of single parameter change, different entropy such as mvMFE, mvMSE and mvMDE are used to analyze how complexity varies with parameter. In the case of two parameters change, the change of complexity is analyzed by the chromatomap which takes two parameters as independent variable, and mvMFE, mvMSE, and mvMDE as the dependent variable when the two parameters change simultaneously. Aiming at the performance problem when the complexity of three-dimensional fractional-order chaotic system is analyzed by mvMFE, mvMSE, and mvMDE, the maximum complexity under single parameter and the detection area under two parameters are used as indicators. The result shows that the performance of mvMDE is the best, and the nonlinear term in the mathematical model of fractional-order chaotic system is positively correlated with the complexity of the system. This will provide a new method for measuring the complexity of fractional-order chaotic system, and lay the basis of theoretical analysis and practical application of fractional chaotic system in the fields of image encryption, sound encryption, image compression-encryption technique, and secure communication.

INDEX TERMS Fractional-order chaotic system, complexity analysis, multivariate multiscale fuzzy entropy, multivariate multiscale sample entropy, multivariate multiscale dispersion entropy.

I. INTRODUCTION

Fractional calculus as a classical mathematical theory has been proposed over 300 years ago [1], [2]. However, due to its long-term lack of application background, its development is slow [3], [4]. In recent years, with the development of computer science and the discovery of more and more fractional-order phenomena, people have done a lot of work in the field of fractional calculus [5]–[7]. Based on the study of integer-order chaotic system, the fractional differential operator is introduced into the system. It is found that when the order is fractional, the system still shows complex chaotic behavior [8]–[10]. Because of its rich dynamic characteristics and potential application value, the research on its dynamic characteristics and application has attracted extensive attention [11]–[13]. It has been known that fractional-order chaotic system has been used in image encryption [14], [15], sound encryption [16], image compression-encryption technique [17]–[19], and secure communication [20]–[22].

Complexity analysis of fractional-order chaotic system is an interesting topic in recent years [23]. How to measure the complexity of fractional-order chaotic system correctly and effectively is the basis of its theoretical analysis and engineering application. The complexity of fractional-order chaotic system refers to the possibility that chaotic sequence is close to random sequence. The larger the complexity value

The associate editor coordinating the review of this manuscript and approving it for publication was Yilun Shang.

is, the closer the sequence is to the random sequence and the higher the corresponding security will be. Entropy measure algorithm is an effective way to analyze the complexity of chaotic system. So far, many entropy measure algorithms such as Shannon entropy [24], fuzzy entropy [25], [26], spectral entropy [27]–[29], permutation entropy [30], [31], approximate entropy [32]–[35] and multiscale permutation entropy [36], have been applied to measure the complexity of chaotic system. Compared with multiscale entropy, multivariate multiscale entropy can observe the dynamic complexity of data in multiple channels [37]. Multivariate multiscale entropy which is used in complexity analysis of fractional-order chaotic system has not been reported, so it is necessary to carry out this research on complexity analysis of fractional-order chaotic system by multivariate multiscale fuzzy entropy (mvMFE), multivariate multiscale sample entropy (mvMSE), multivariate multiscale dispersion entropy (mvMDE).

In order to solve the complexity problem of three-dimensional fractional-order chaotic system, complexity analysis method of three-dimensional fractional-order chaotic system based on mvMFE, mvMSE and mvMDE is proposed. In single parameter and double parameters respectively, two three-dimensional fractional-order chaotic systems are analyzed by the proposed method. The experimental results show that the performance of mvMDE is the best, and the complexity of the three-dimensional fractional-order chaotic system is positively correlated with the existence of the nonlinear term.

The rest of this paper is arranged as follows. In Section II, the definitions of the fractional derivatives are presented. In Section III, two types of fractional-order chaotic systems are presented. In Section IV, complexity analysis of three-dimensional fractional-order chaotic system based on entropy theory is proposed, and its performance is studied. Finally, discussion and conclusions are summarized in Section V.

II. THE DEFINITIONS OF THE FRACTIONAL DERIVATIVES

In recent years, fractional-order differential operators are introduced into nonlinear dynamical system, and the study of chaos in fractional-order nonlinear dynamical systems becomes a hot topic. At present, there are many definitions of the fractional derivatives, including Grünwald-Letnikov (G-L) definition [38], [39], Riemann-Liouville (R-L) definition [40], [41] and Caputo definition [42], [43].

(1) The Grünwald-Letnikov fractional differential is defined as [44]:

$$ {}_aD_t^q f(t) = \frac{d^q f(t)}{d(t-a)^q} = \lim_{N\to\infty}[\frac{t-a}{N}]^{-q} \times \sum_{j=0}^{N-1}(-1)^j \binom{q}{j} f(t-j[\frac{t-a}{N}]) \quad (1) $$

where, ${}_aD_t^q$ is the fractional calculus operator. ${}_aD_t^q$ can simultaneously represent the derivative of the fractional order and the integral of the fractional order. When $q > 0$, ${}_aD_t^q$ represents the derivative. When $q < 0$, ${}_aD_t^q$ represents the integral.

(2) The Riemann-Liouville fractional differential is defined as [45]:

$$ {}_aD_t^q f(t) = \begin{cases} \frac{1}{\Gamma(-q)}\int_a^t (t-\tau)^{-q-1} f(\tau)d\tau & q<0 \\ f(t) & q=0 \\ D^n[{}_aD_t^{q-n} f(t)] & q>0 \end{cases} \quad (2) $$

The power series and constant of q-order differential are defined respectively as:

$$ D_{t_0}^q t^r = \frac{\Gamma(r+1)}{\Gamma(r+1-q)}(t-t_0)^{r-q} \quad (3) $$

$$ D_{t_0}^q C = \frac{C}{\Gamma(1-q)}(t-t_0)^{-q} \quad (4) $$

where $\Gamma(\cdot)$ is the Gamma function.

(3) The Caputo fractional differential is defined as [46]:

$$ {}_aD_{t_0}^q f(t) = \begin{cases} \frac{1}{\Gamma(m-q)}\int_0^t \frac{f(m)(\tau)d\tau}{(t-\tau)^{q+1-m}} & m-1<q<m \\ \frac{d^m}{dt^m} f(t) & q=m \end{cases} \quad (5) $$

The power series and constant of q-order differential are defined respectively as:

$$ D_{t_0}^q t^r = \frac{\Gamma(r+1)}{\Gamma(r+1-q)}(t-t_0)^{r-q} \quad (6) $$

$$ D_{t_0}^q C = 0 \quad (7) $$

Among them, Caputo definition is more utilized in practical application research due to its more clear physical significance and easy implementation in engineering [31]. So the Caputo definition is used in this paper.

III. TWO TYPES OF FRACTIONAL-ORDER CHAOTIC SYSTEMS

A. FRACTIONAL-ORDER A CHAOTIC SYSTEM

In 2013, Jafari [47] *et al.* proposed a series of three-dimensional chaotic systems. One of the integer-order chaotic systems is selected, which is called integer-order a chaotic system in the following for the convenience of presentation. Its mathematical model is:

$$ \begin{cases} \frac{dx}{dt} = y \\ \frac{dy}{dt} = -x + yz \\ \frac{dz}{dt} = -x - \text{axy-bxz} \end{cases} \quad (8) $$

On the basis of integer-order a chaotic system, fractional operator is introduced, and fractional-order a chaotic system can be obtained. Its mathematical model is:

$$ \begin{cases} D_{t_0}^q x_1 = x_2 \\ D_{t_0}^q x_2 = -x_1 + x_2 x_3 \\ D_{t_0}^q x_3 = -x_1 - a x_1 x_2 - b x_1 x_3 \end{cases} \quad (9) $$

The most common methods for solving fractional-order chaotic systems are frequency domain method (FDM) [48], [49], predictor-corrector method (PCM) [50], [51], and Adomian decomposition method (ADM) [52], [53]. As a numerical resolution algorithm, ADM is more accurate than FDM and PCM numerically and theoretically [53]. So, ADM is used to solve fractional-order chaotic system. The analyzed data set is a data set obtained by numerical analysis by ADM. When $a = 15, b = 1$, initial value $(x0, y0, z0) = (0, 0.5, 0.5)$, order $q = 0.999$, the phase trajectory diagram of each plane is shown in Figure 1. The purpose of choosing $q = 0.999$ in this paper is to verify the correctness of Adomian decomposition method. When simulating in MATLAB, the order q can be chosen at will.

B. FRACTIONAL-ORDER B CHAOTIC SYSTEM

A class of integer-order b chaotic systems with a structure similar to integer-order a chaotic systems [47] is introduced. Its mathematical model is:

$$\begin{cases} \dfrac{dx}{dt} = y \\ \dfrac{dy}{dt} = -x + yz \\ \dfrac{dz}{dt} = x^2 - \text{axy-bxz} \end{cases} \tag{10}$$

On the basis of the integer-order b chaotic system, fractional operator is introduced, and fractional-order b chaotic system can be obtained. Its mathematical model is

$$\begin{cases} D_{t_0}^q x_1 = x_2 \\ D_{t_0}^q x_2 = -x_1 + x_2 x_3 \\ D_{t_0}^q x_3 = x_1^2 - a x_1 x_2 - b x_1 x_3 \end{cases} \tag{11}$$

Comparison formula (9) and formula (11), we can clearly see that the fractional-order b chaotic system has only one more nonlinear term compared with the fractional-order a chaotic system, and other structures are the same. Therefore, these two chaotic systems are chosen for convenience of comparison to explore the influence of nonlinear term on the complexity of fractional-order chaotic system.

In this paper, ADM is used to numerically analyze fractional-order chaotic system. Only the numerical results of fractional-order b chaotic system are obtained here, and the fractional-order a chaotic system is similar and will not be described again. After decomposing nonlinear term x_2x_3 and nonlinear term $x_1^2 - ax_1x_2 - bx_1x_3$, we can get:

$$\begin{cases} A_2^0 = x_2^0 x_3^0 \\ A_2^1 = x_2^1 x_3^0 + x_2^0 x_3^1 \\ A_2^2 = x_2^2 x_3^0 + x_2^1 x_3^1 + x_2^0 x_3^2 \\ A_2^3 = x_2^3 x_3^0 + x_2^2 x_3^1 + x_2^1 x_3^2 + x_2^0 x_3^3 \\ A_2^4 = x_2^4 x_3^0 + x_2^3 x_3^1 + x_2^2 x_3^2 + x_2^1 x_3^3 + x_2^0 x_3^4 \\ A_2^5 = x_2^5 x_3^0 + x_2^4 x_3^1 + x_2^3 x_3^2 + x_2^2 x_3^3 + x_2^1 x_3^4 + x_2^0 x_3^5 \end{cases}$$

$$\begin{cases} A_3^0 = x_1^0 x_1^0 + a(-x_1^0 x_2^0) - b x_1^0 x_3^0 \\ A_3^1 = 2x_1^1 x_1^0 + a(-x_1^1 x_2^0 - x_1^0 x_2^1) - b(x_1^1 x_3^0 + x_1^0 x_3^1) \\ A_3^2 = 2x_1^2 x_1^0 + x_1^1 x_1^1 + a(-x_1^2 x_2^0 - x_1^1 x_2^1 - x_1^0 x_2^2) \\ -b(x_1^2 x_3^0 + x_1^1 x_3^1 + x_1^0 x_3^2) \\ A_3^3 = 2x_1^3 x_1^0 + 2x_1^2 x_1^1 + a(-x_1^3 x_2^0 - x_1^2 x_2^1 - x_1^1 x_2^2 - x_1^0 x_2^3) \\ -b(x_1^3 x_3^0 + x_1^2 x_3^1 + x_1^1 x_3^2 + x_1^0 x_2^3) \\ A_3^4 = 2x_1^4 x_1^0 + 2x_1^3 x_1^1 + x_1^2 x_1^2 + a(-x_1^4 x_2^0 - x_1^3 x_2^1 \\ -x_1^2 x_2^2 - x_1^1 x_2^3 - x_1^0 x_2^4) - b(x_1^4 x_3^0 + x_1^3 x_3^1 + x_1^2 x_3^2 \\ +x_1^1 x_3^3 - x_1^0 x_3^4) \\ A_3^5 = 2x_1^5 x_1^0 + 2x_1^4 x_1^1 + 2x_1^3 x_1^2 + a(-x_1^5 x_2^0 \\ -x_1^4 x_2^1 - x_1^3 x_2^2 - x_1^2 x_2^3 - x_1^1 x_2^4 - x_1^0 x_2^5) - b(x_1^5 x_3^0 + x_1^4 x_3^1 \\ +x_1^3 x_3^2 + x_1^2 x_3^3 - x_1^1 x_3^4 - x_1^0 x_3^5) \end{cases}$$

The collation result of derivation process are as follows:

$$\begin{cases} c_1^1 = c_2^0 \\ c_2^1 = [-c_1^0 + c_2^0 c_3^0] \\ c_3^1 = [c_1^0 c_1^0 - a c_1^0 c_2^0 - b c_1^0 c_3^0] \end{cases}$$

$$\begin{cases} c_1^2 = c_2^1 \\ c_2^2 = [-c_1^1 + c_2^1 c_3^0 + c_2^0 c_3^1] \\ c_3^2 = [2c_1^1 c_1^0 + a(-c_1^1 c_2^0 - c_1^0 c_2^1) + b(c_1^1 c_3^0 - c_1^0 c_3^1)] \end{cases}$$

$$\begin{cases} c_1^3 = c_2^2 \\ c_2^3 = [-c_1^2 + c_2^2 c_3^0 + c_2^1 c_3^1 \dfrac{\Gamma(2q+1)}{\Gamma(q+1)^2} + c_2^0 c_3^2] \\ c_3^3 = [2c_1^2 c_1^0 + c_1^1 c_1^1 \dfrac{\Gamma(2q+1)}{\Gamma(q+1)^2} \\ +a(-c_1^2 c_2^0 - c_1^0 c_2^1 \dfrac{\Gamma(2q+1)}{\Gamma(q+1)^2} - c_1^0 c_2^2) \\ +b(-c_1^2 c_3^0 - c_1^1 c_3^1 \dfrac{\Gamma(2q+1)}{\Gamma(q+1)^2}) - c_1^0 c_3^2] \end{cases}$$

$$\begin{cases} c_1^4 = c_2^3 \\ c_2^4 = [-c_1^3 + c_2^3 c_3^0 + (c_2^2 c_3^1 + c_2^1 c_3^2) \\ \dfrac{\Gamma(3q+1)}{\Gamma(q+1)\Gamma(2q+1)} + c_2^0 c_3^3] \\ c_3^4 = [2c_1^3 c_1^0 + 2c_1^2 c_1^1 \dfrac{\Gamma(3q+1)}{\Gamma(q+1)\Gamma(2q+1)} \\ +a(-c_1^3 c_2^0 - (c_1^2 c_2^1 + c_1^1 c_2^2) \dfrac{\Gamma(3q+1)}{\Gamma(q+1)\Gamma(2q+1)} - c_1^0 c_2^3) \\ +b(-c_1^3 c_3^0 - (c_1^2 c_3^1 + c_1^1 c_3^2) \dfrac{\Gamma(3q+1)}{\Gamma(q+1)\Gamma(2q+1)}) - c_1^0 c_3^3] \end{cases}$$

$$\begin{cases} c_1^5 = c_2^4 \\ c_2^5 = [-c_1^4 + c_2^4 c_3^0 + (c_2^3 c_3^1 + c_2^1 c_3^3) \dfrac{\Gamma(4q+1)}{\Gamma(q+1)\Gamma(3q+1)} \\ +c_2^2 c_3^2 \dfrac{\Gamma(4q+1)}{\Gamma(2q+1)^2} + c_2^0 c_3^4] \\ c_3^5 = [2c_1^4 c_1^0 + 2c_1^3 c_1^1 \dfrac{\Gamma(4q+1)}{\Gamma(q+1)\Gamma(3q+1)} \\ +c_1^2 c_1^2 \dfrac{\Gamma(4q+1)}{\Gamma(2q+1)^2} + a(-c_1^4 c_2^0 - (c_1^3 c_2^1 + c_1^1 c_2^3) \\ \dfrac{\Gamma(4q+1)}{\Gamma(q+1)\Gamma(3q+1)} - c_1^2 c_2^2 \dfrac{\Gamma(4q+1)}{\Gamma(2q+1)^2} \\ -c_1^0 c_2^4) + b(-c_1^4 c_3^0 - (c_1^3 c_3^1 + c_1^1 c_3^3) \\ \dfrac{\Gamma(4q+1)}{\Gamma(q+1)\Gamma(3q+1)}) - c_1^2 c_3^2 \dfrac{\Gamma(4q+1)}{\Gamma(2q+1)^2} - c_1^0 c_3^4] \end{cases}$$

$$\begin{cases} c_1^6 = c_2^5 \\ c_2^6 = -c_1^5 + c_2^5 c_3^0 + (c_2^4 c_3^1 + c_2^1 c_3^4)\dfrac{\Gamma(5q+1)}{\Gamma(q+1)\Gamma(4q+1)} \\ +(c_2^3 c_3^2 + c_2^2 c_3^3)\dfrac{\Gamma(5q+1)}{\Gamma(2q+1)\Gamma(3q+1)} + c_2^0 c_3^5 \\ c_3^6 = 2c_1^5 c_1^0 + 2c_1^4 c_1^1 \dfrac{\Gamma(5q+1)}{\Gamma(q+1)\Gamma(4q+1)} \\ +2c_1^3 c_1^2 \dfrac{\Gamma(5q+1)}{\Gamma(2q+1)\Gamma(3q+1)} - a(c_1^5 c_2^0 + (c_1^4 c_2^1 + c_1^1 c_2^4) \\ \dfrac{\Gamma(5q+1)}{\Gamma(q+1)\Gamma(4q+1)} + (c_1^3 c_2^2 + c_1^2 c_2^3)\dfrac{\Gamma(5q+1)}{\Gamma(2q+1)\Gamma(3q+1)} \\ +c_1^0 c_2^5) - b(c_1^5 c_3^0 + (c_1^4 c_3^1 + c_1^1 c_3^4) \\ \dfrac{\Gamma(5q+1)}{\Gamma(q+1)\Gamma(4q+1)} + (c_1^3 c_3^2 + c_1^2 c_3^3)\dfrac{\Gamma(5q+1)}{\Gamma(2q+1)\Gamma(3q+1)} \\ +c_1^0 c_3^5) \end{cases}$$

When $a = 18, b = 1$, initial value $(x0, y0, z0) = (0, -0.4, 0.5)$, order $q = 0.999$, the phase trajectory diagram of each plane phase is shown in Figure 2.

IV. COMPLEXITY ANALYSIS OF THREE-DIMENSIONAL FRACTIONAL-ORDER CHAOTIC SYSTEM BASED ON ENTROPY THEORY

A. COMPLEXITY ANALYSIS OF THREE-DIMENSIONAL FRACTIONAL-ORDER CHAOTIC SYSTEM BASED ON MULTIVARIATE MULTISCALE FUZZY ENTROPY

1) MULTIVARIATE MULTISCALE FUZZY ENTROPY ALGORITHM

Multivariate multiscale fuzzy entropy (mvMFE) [54] is not easy to cause data loss when analyzing higher scale and shorter data, and it has a low dependence on the threshold, so it has a strong advantage compared with fuzzy entropy. The calculation steps are as follows:

(1) For a multivariate signal $\{x_{k,i}\}_{i=1}^{N}, k = 1, 2, \ldots, p$ containing p sub-signal of length L, a new time series can be obtained by coarse-graining at any scale $\tau = 1, 2, \ldots, (\tau \geq 1)$:

$$y_{k,j}^{(\tau)} = \frac{1}{\tau} \sum_{i=(j-1)\tau+1}^{j\tau} x_{k,i} \tag{12}$$

(2) Reconstruct multiple phase space of $y_{k,j}^{(\tau)}$, and get:

$$X_m(i) = [x_{1,i}, \ldots, x_{1,i+(m_1-1)_{t_1}}, \ldots, x_{p,i}, \ldots, x_{p,i+(m_p-1)_{t_p}}] \tag{13}$$

where, $M = [m_1, m_2, \ldots, m_p]$ and $t = [t_1, t_2, \ldots, t_p]$ are the embedding dimension and delay time respectively, $n = \max\{M\} \times \max\{t\}, i = 1, 2, \ldots, L - n$.

(3) Use the maximum norm to define the distance between any two phase spaces $X_m(i)$ and $X_m(j)$. When $d[X_m(i), X_m(j)] > r$, find all the values N_i of $A(x)$. Calculate the sum of M_i and N_i:

$$E_i = M_i + N_i \tag{14}$$

Solve the ratio of E_i and $L-n-1$, and obtain the frequency:

$$\Phi_i^m(r) = \frac{1}{L-n-1} E_i \tag{15}$$

The conditional probability at this time is:

$$\Phi_i^m(r) = \frac{1}{L-n} \sum_{i=1}^{L-n} \Phi_i^m(r) \tag{16}$$

According to the above derivation, when extended to $m+1$ dimensions, the conditional probability is:

$$\Phi_i^{m+1}(r) = \frac{1}{L-n} \sum_{i=1}^{L-n} \Phi_i^{m+1}(r) \tag{17}$$

(4) Find the natural logarithm of $\Phi_i^m(r)$ and $\Phi_i^{m+1}(r)$, and get multivariate multiscale fuzzy entropy:

$$mvMFE = \ln\left[\frac{\Phi_i^m(r)}{\Phi_i^{m+1}(r)}\right] \tag{18}$$

2) COMPLEXITY ANALYSIS OF THREE-DIMENSIONAL FRACTIONAL-ORDER CHAOTIC SYSTEM BASED ON MULTIVARIATE MULTISCALE FUZZY ENTROPY

When order $q = 0.96$, system parameters $a \in (12, 20)$, $b = 1, N = 15000$, complexity of fractional-order a chaotic system is shown in Figure 3(a). The complexity value is the exact value obtained by using vernier caliper tool in simulation diagram. When $a = 13.84$, the complexity reaches its maximum value. When $a \in (12, 15.2)$, the complexity is in a violent oscillation state with the increase of parameter a. When $a \in (15.2, 20)$, the complexity tends to be stable and no longer changes. When the parameters $a = 15, b = 1$, $q \in [0.2, 1]$, the complexity of fractional-order a chaotic system is shown in Figure 3(b). When $q = 0.5813$, the complexity reaches its maximum value. When $q \in (0.2, 0.5813)$, the complexity almost tends to 0 and is smooth and stable. As the order increases until $q = 1$, the complexity tends to decrease. When the system parameters $a = 15, q = 0.96$, $b \in (0.2, 1.2)$, the complexity of fractional-order a chaotic system is shown in Figure 3(c). When the parameter $b = 0.6$, the complexity reaches its maximum value. When the parameter $b \in (0.2, 0.6)$, the complexity increases slowly. Until $b = 1.2$, the complexity is basically stable with slow oscillation.

When order $q = 0.96$, system parameters $a \in (14, 22)$, $b = 1$, and $N = 15000$, complexity of fractional-order b chaotic system is shown in Figure 4(a). When $a = 17.71$, the complexity reaches its maximum value. When $a \in (14, 15.79)$, the complexity increases and then stays in a violent oscillation state. Until $a = 22$, the complexity no longer changes significantly and is in a smooth and stable state. When $a = 18, b = 1, q \in (0.2, 1)$, complexity of the fractional-order b chaotic system is shown in Figure 4(b). When $q = 0.4187$, the complexity reaches its maximum, and the overall trend is that the complexity first increases to the maximum and then decreases as the order q increases. When $a = 18, q = 0.96, b \in (0.2, 1.2)$, the complexity of fractional-order b chaotic system is shown in Figure 4(c). When $a \in (0.22, 0.38)$, the complexity is extremely small and almost tends to 0. With the increase of parameter b until

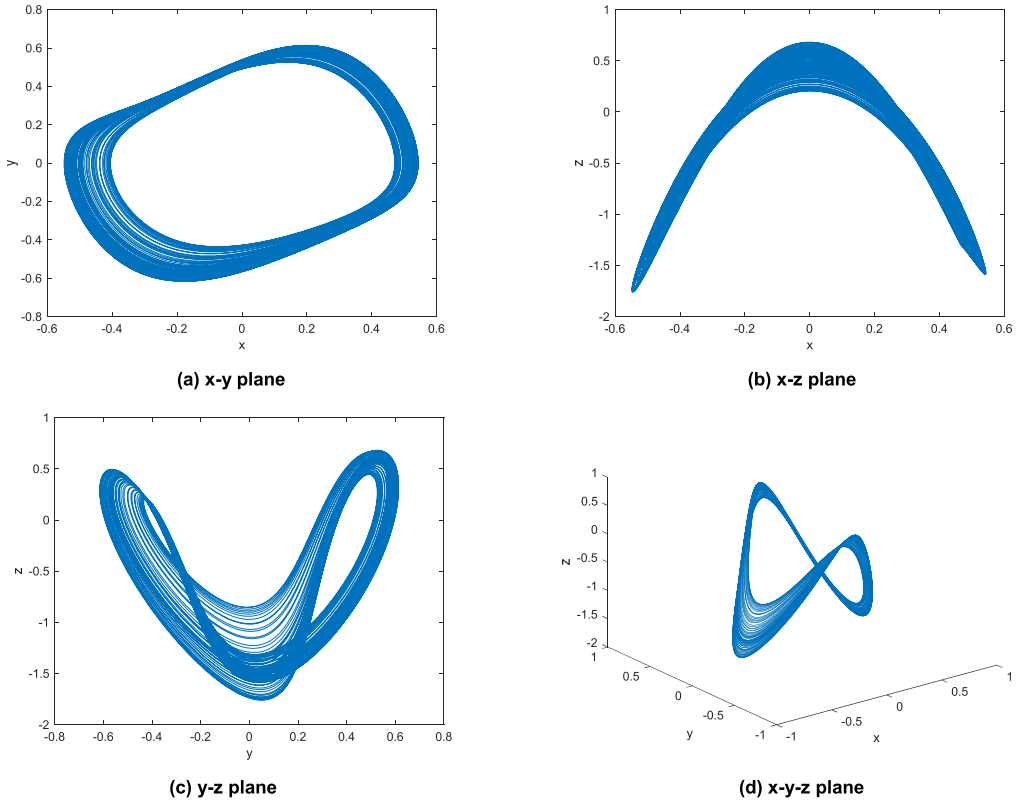

FIGURE 1. Phase trajectory diagram of fractional-order *a* chaotic system.

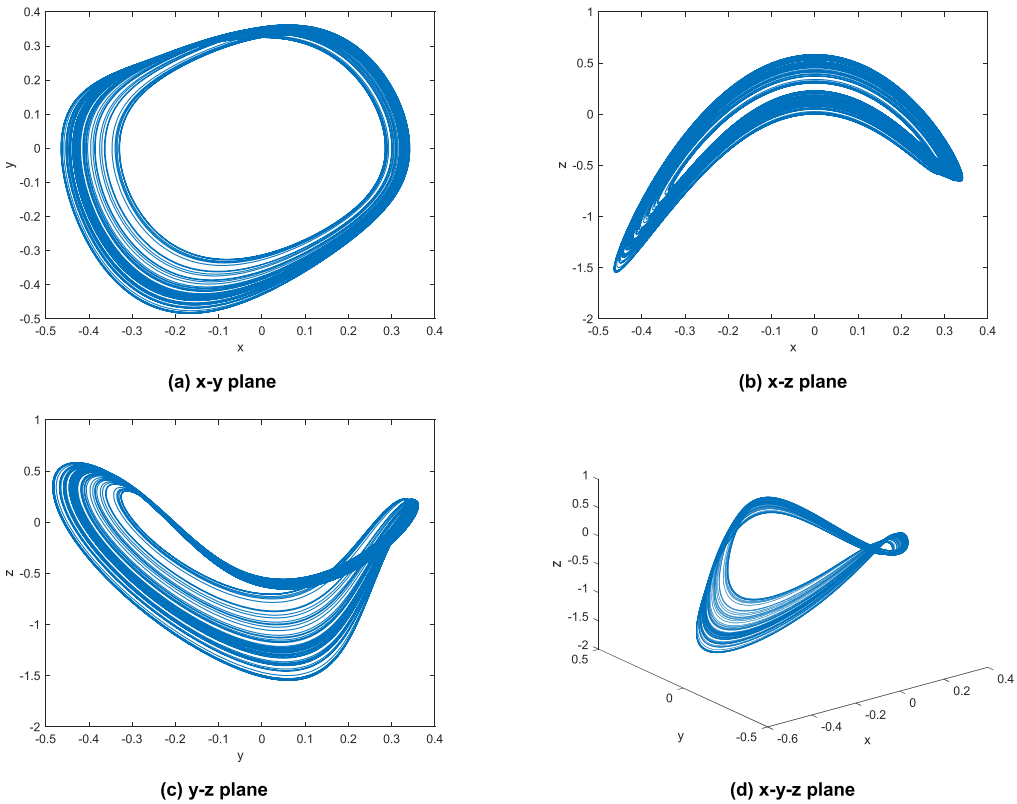

FIGURE 2. Phase trajectory diagram of fractional-order *b* chaotic system.

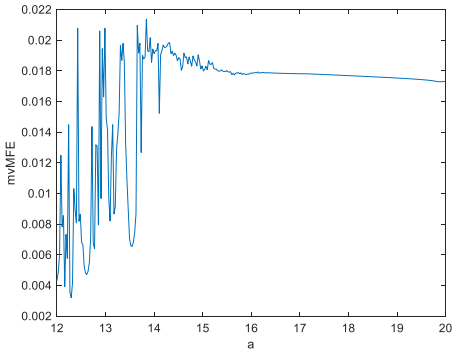

(a) Change trend of complexity with parameter a

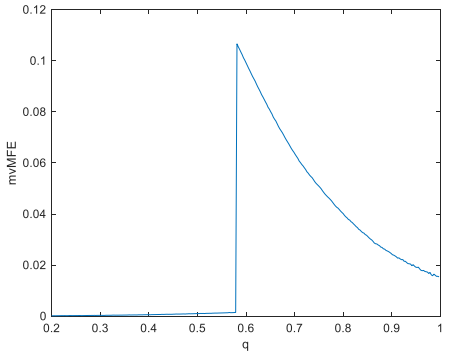

(b) Change trend of complexity with order q

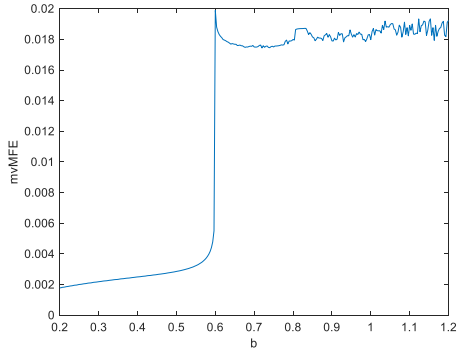

(c) Change trend of complexity with parameter b

FIGURE 3. Change trend of mvMFE complexity of fractional-order *a* chaotic system under single parameter.

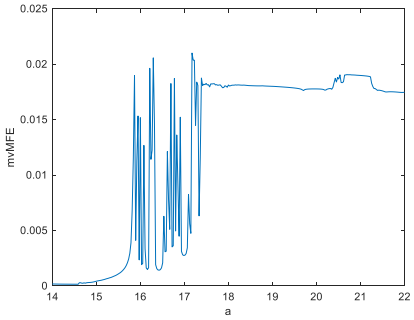

(a) Change trend of complexity with parameter a

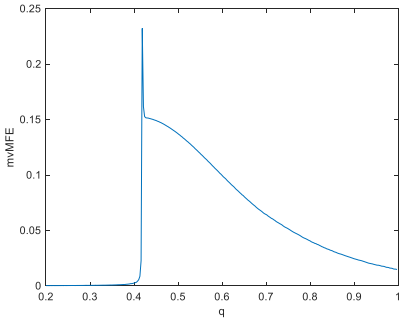

(b) Change trend of complexity with order q

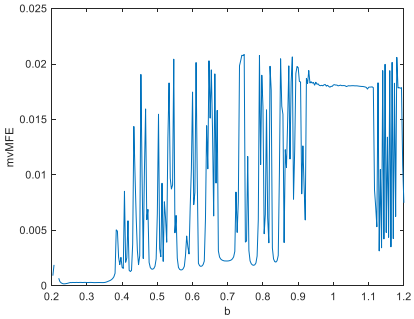

(c) Change trend of complexity with parameter b

FIGURE 4. Change trend of mvMFE complexity of fractional-order *b* chaotic system under single parameter.

$b = 0.9333$, the complexity change trend is violent oscillation. When $b = 0.7467$, the complexity reaches the maximum value. When $b \in (0.9333, 1.11)$, the complexity basically no longer changes and tends to stabilize. Until $b = 1.2$, the complexity oscillates violently.

For fractional-order a chaotic system, when $a \in (12, 20)$ and $q \in (0.2, 1)$, the chromatogram of the complexity change is shown in Figure 5(a). When $q \in (0.576, 0.5973)$ and $a \in (12, 20)$, the color is the darkest, that is, the complexity is the largest. As the order q increases, the overall complexity trend shows a grid-like decrease. When $b \in (0.2, 1.2)$, and $q \in (0.2, 1)$, the chromatogram of the complexity change is shown in Figure 5(b). The overall shape is a fan, and the bottom is $q \in (0.5733, 0.5973)$. When $b \in (0.9267, 1.2)$, the complexity is the largest, and the overall change trend is to decrease with the increase of the order q. When $a \in (12, 20)$ and $b \in (0.2, 1.2)$, the chromatogram of the complexity change is shown in Figure 5(c). It can be clearly seen that the entire area is divided into the lower part and the upper part. The lighter overall color of the lower part indicates that the complexity of this area is low, and the darker overall color of the upper part means higher complexity.

For fractional-order b system, when $a \in (14, 22)$ and $q \in (0.2, 1)$, the complexity change chromatogram is shown in Figure 6(a). When $q > 0.3733$, the complexity decreases with the increase of q, and the complexity of the bottom area is the largest. When $b \in (0.2, 1.2)$ and $q \in (0.2, 1)$, the complexity change chromatogram is shown in Figure 6(b). When $q > 0.4107$, the complexity decreases with the increase of q. The area with the largest complexity is at the bottom. When $a \in (14, 22)$ and $b \in (0.2, 1.2)$, the complexity change chromatogram is shown in Figure 6(c), and the complexity is mainly concentrated in the upper right area and the boundary is the most complicated.

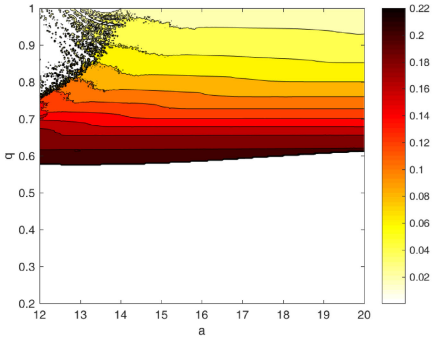

(a) Change trend of complexity with parameter a and q

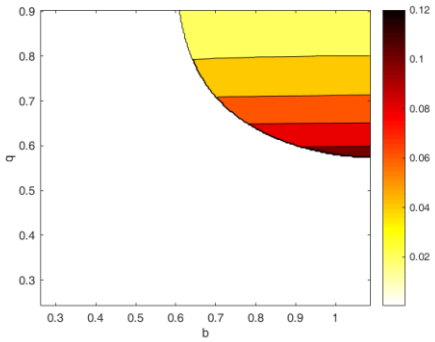

(b) Change trend of complexity with parameter b and q

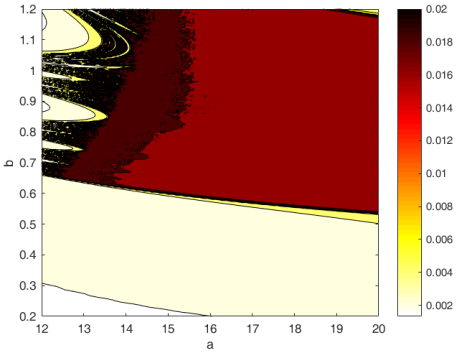

(c) Change trend of complexity with parameter a and b

FIGURE 5. mvMFE complexity chromatogram of fractional-order a chaotic system.

B. COMPLEXITY ANALYSIS OF THREE-DIMENSIONAL FRACTIONAL-ORDER CHAOTIC SYSTEM BASED ON MULTIVARIATE MULTISCALE SAMPLE ENTROPY

1) MULTIVARIATE MULTISCALE SAMPLE ENTROPY ALGORITHM

Multivariate multiscale sample entropy (mvMSE) [55] can evaluate the complexity of multi-channel data on multiple time scales and obtain more accurate results, and has a high degree of freedom. The main calculation steps are as follows:

(1) The time series $\{x_1, x_2, \ldots, x_N\}$ is coarse-grained according to formula (19), and the time series is continuously coarse-grained under the time scale factor τ. Get the coarse-grained data $y_j^{(\tau)}$:

$$y_j^{(\tau)} = \frac{1}{\tau} \sum_{i=(j-1)\tau+1}^{j\tau} x_i (1 \le j \le N/\tau) \tag{19}$$

(2) For each scale τ, calculate MSE of the coarse-grained data $y_j^{(\tau)}$, and for p time series $\left\{x_{k,i}\right\}_{i=1}^{N}, k = 1, 2, \ldots, p$, generate a composite delay vector as:

$$X_m(i) = [x_{1,i}, x_{1,i+\tau_1}, \ldots, x_{1,i+(m_1-1)_{\tau_1}}, \ldots, x_{p,i}, x_{p,i+\tau_p}, \ldots, x_{p,i+(m_p-1)_{\tau_p}}] \tag{20}$$

$$d[X_m(i), X_m(j)] = \max_{l=1,2,\ldots,m} \{|y^{\tau}(i+l-1) - y^{\tau}(j+l-1)|\} \tag{21}$$

where $X_m(i)$ is the multivariate delay vector, $M = [m_1, m_2, \ldots, m_p]$ is the embedding vector, and $\tau = [\tau_1, \tau_2, \ldots, \tau_p]$ is the delay vector.

(3) Generate $N - n$ composite delay vectors X_m according to the formula (20), and substitute them into the formula (21) to calculate the distance between the $X_m(i)$ and $X_m(j)$ vectors.

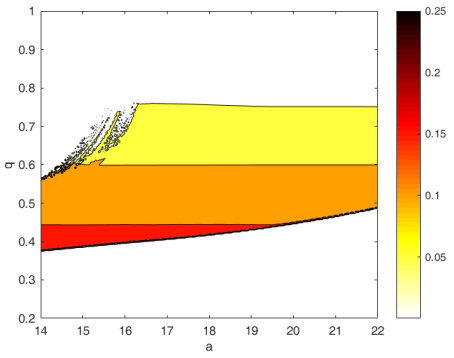

(a) Change trend of complexity with parameter a and q

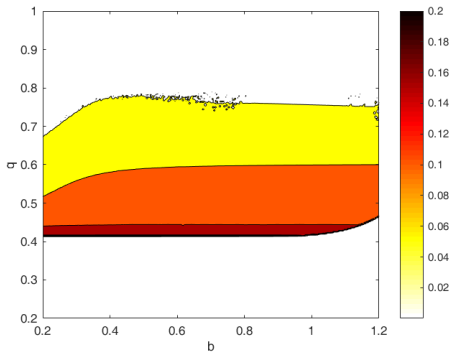

(b) Change trend of complexity with parameter b and q

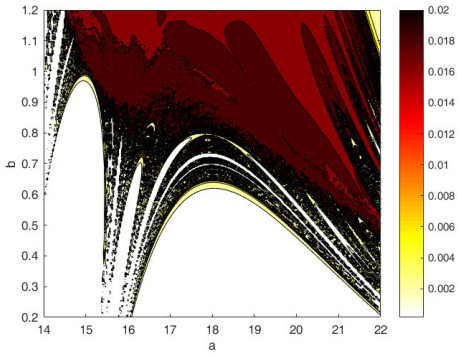

(c) Change trend of complexity with parameter a and b

FIGURE 6. mvMFE complexity chromatogram of fractional-order *b* chaotic system.

(4) Count the number P_i of $d[X_m(i), X_m(j)] \leq r(j \neq i)$, and its probability is:

$$P_i^m(r) = \frac{P_i}{N - n - 1} \tag{22}$$

The average of P_i is:

$$P^m(r) = \frac{1}{N - n} \sum_{i=1}^{N-n} P_i^m(r) \tag{23}$$

where $n = \max\{M_m\} \times \max\{\tau\}$.

(5) Expand $X_m(i)$ dimension, that is, make its dimension be $m + 1$. $p \times (N - n)$ multivariate delay vectors $X_m(i)$ can be obtained in the $m + 1$ dimensional space.

(6) P_i with embedded vector $M_{m+1}(i)$ can be obtained, and its average value is:

$$P^{m+1}(r) = \frac{1}{p(N - n)} \sum_{i=1}^{p(N-n)} P_i^{m+1}(r) \tag{24}$$

(7) $P^m(r)$ and $P^{m+1}(r)$ respectively represent the conditional probability of variables similarity in the m dimensional and $m + 1$ dimensional. mvMSE can be expressed as:

$$mvMSE = -\ln[\frac{P^{m+1}(r)}{P^m(r)}] \tag{25}$$

2) COMPLEXITY ANALYSIS OF THREE-DIMENSIONAL FRACTIONAL-ORDER CHAOTIC SYSTEM BASED ON MULTIVARIATE MULTISCALE SAMPLE ENTROPY

When order $q = 0.96$, system parameters $a \in (12, 20)$, $b = 1$, $N = 15000$, complexity of the fractional-order a chaotic system is shown in Figure 7(a). When $a \in (12, 14.21)$, the complexity starts to vibrate violently with the increase of parameter a. When $a = 13.84$, the complexity reaches the maximum, and the complexity gradually stabilizes until $a = 20$. When the parameters $a = 15$, $b = 1$, and $q \in (0.2, 1)$, complexity of the fractional-order a chaotic system is shown in Figure 7(b). When $q \in (0.2, 0.5787)$, the complexity is relatively low and basically tends to 0. When $q = 0.5813$, the complexity rises linearly to reach the maximum value of the area. Until $q = 1$, the complexity gradually decreases with the increase of order q. When system parameters $a = 15$, $q = 0.96$, and $b \in (0.2, 1.2)$, complexity of the fractional-order a chaotic system is shown in Figure 7(c). When $b \in (0.2, 0.5967)$, complexity is low, and it is in a smooth state. When $b = 0.6$, it increases sharply and reaches the maximum until the complexity is in an oscillating state when $b = 1.2$.

When order $q = 0.96$, system parameters $a \in (14, 22)$, $b = 1$, $N = 15000$, complexity of the fractional-order b chaotic system is shown in Figure 8(a). When $a \in (14, 15.57)$, the complexity is low and basically tends to 0. When $a \in (15.57, 17.39)$, the complexity fluctuates sharply and reaches

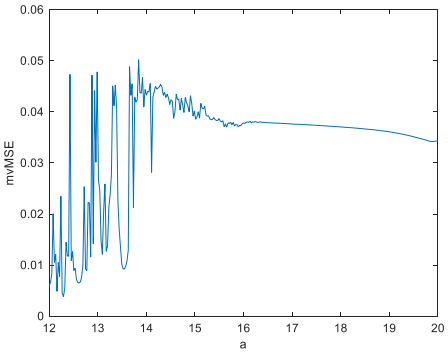

(a) Change trend of complexity with parameter a

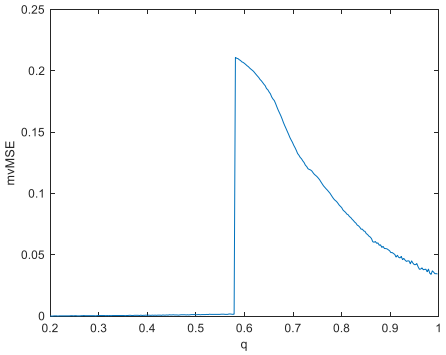

(b) Change trend of complexity with order q

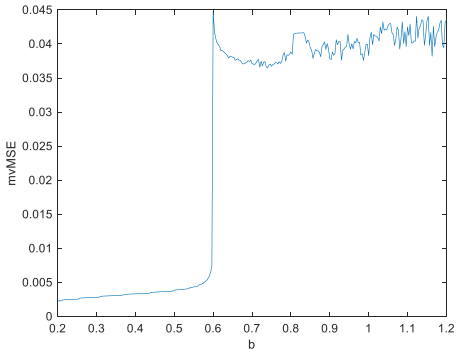

(c) Change trend of complexity with parameter b

FIGURE 7. Change trend of mvMSE complexity of fractional-order *a* chaotic system under single parameter.

the maximum when $a = 17.17$. When $a \in (17.39, 20.35)$, complexity no longer has obvious changes and tends to be stable. Until $a = 22$, the complexity first increases, then basically remains unchanged, and then gradually decreases. When $a = 18$, $b = 1$, $q \in (0.2, 1)$, complexity of the fractional-order b chaotic system is shown in Figure 8(b). When $q \in (0.2, 0.4133)$, the complexity is basically a straight line tending to 0. When $q = 0.4187$, the complexity increases sharply and reaches the maximum value until $q = 1$ when the complexity decreases as a whole. When system parameters $a = 18$, $q = 0.96b \in (0.2, 1.2)$, complexity of the fractional-order b chaotic system is shown in Figure 8(c). When $b \in (0.2, 0.3567)$ the complexity basically tends to 0. When $b \in (0.3567, 0.9367)$, the complexity changes sharply in an oscillating state and reaches the maximum value at $b = 0.7467$. When $b \in (0.9367, 1.103)$, the complexity changes from a severely oscillating state to a stationary state. When $b \in (1.103, 1.2)$, the complexity is in an oscillating state and the oscillation frequency is faster than that when $b \in (0.3567, 0.9367)$.

For fractional-order a chaotic system, when $a \in (12, 20)$ and $q \in (0.2, 1)$, the chromatogram of complexity change is shown in Figure 9(a). The overall discrimination is better and the complexity of this area is the largest when $q \in (0.576, 0.616)$, and the overall complexity decreases as the order q increases when $q > 0.576$. When $b \in (0.2, 1.2)$ and $q \in (0.2, 1)$, the chromatogram of complexity change is shown in Figure 9(b). The overall discrimination is better and the complexity is the largest when $b \in (0.8734, 1.2)$ and $q \in (0.5698, 0.6181)$. When $q > 0.5698$, as the number q increases, the complexity decreases. When $a \in (12, 20)$ and $b \in (0.2, 1.2)$, the chromatogram of complexity change is shown in Figure 9(c). The complexity is the largest at the left boundary and decreases as the system parameter a increases.

For fractional-order b chaotic system, when $a \in (14, 22)$ and $q \in (0.2, 1)$, the chromatogram of complexity change is shown in Figure 10(a). The obvious colors at the bottom edge and the upper left edge are darker than that in other areas, indicating that this area has the deepest complexity. When $q > 0.3733$, the complexity decreases with the increase of the order q and the discrimination is better. When $b \in (0.2, 1.2)$ and $q \in (0.2, 1)$, the chromatogram of complexity change is shown in Figure 10(b). It is obvious that the overall discrimination is poorer than that in Figure 10(a), and the area with the largest complexity is at the bottom. When $q > 0.4133$, the complexity decreases with the increase of the order q. When $a \in (14, 22)$ and $b \in (0.2, 1.2)$, the chromatogram of complexity change is shown in Figure 10(c). It can be seen that the complexity change trend is more complicated and has no specific rules. The color is the darkest at the edge,

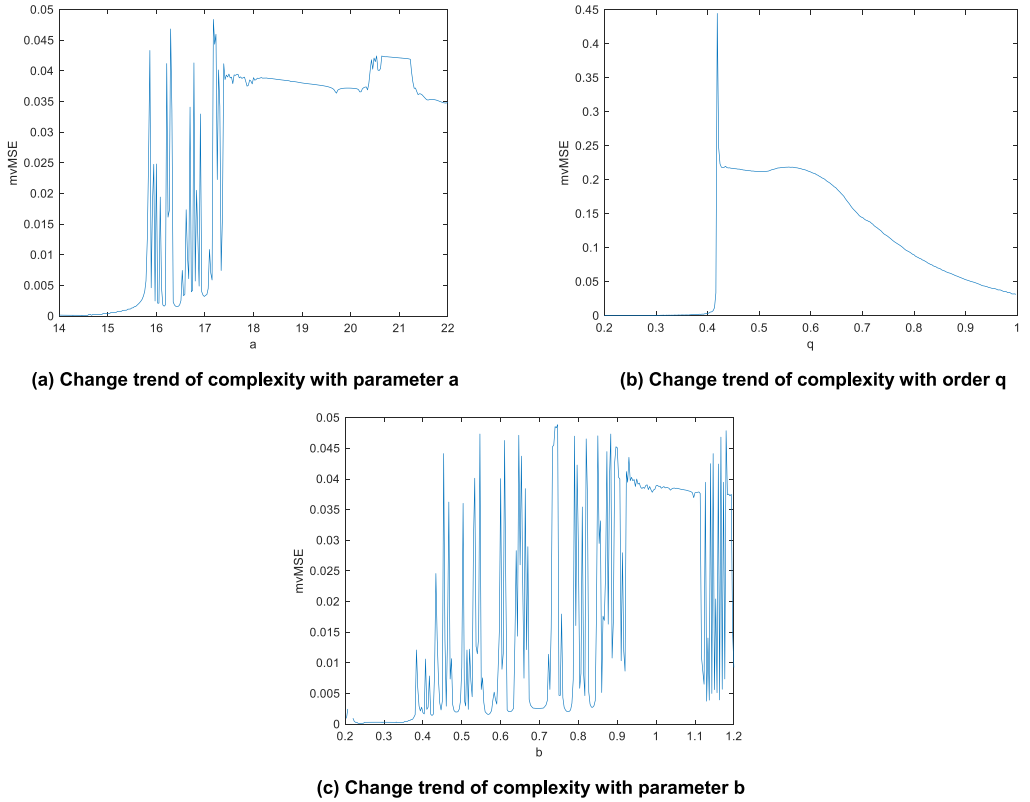

(a) Change trend of complexity with parameter a

(b) Change trend of complexity with order q

(c) Change trend of complexity with parameter b

FIGURE 8. Change trend of mvMSE complexity of fractional-order *b* chaotic system under single parameter.

that is, the complexity is the largest in the area. And the complexity on the left is greater than the complexity on the right.

C. COMPLEXITY ANALYSIS OF THREE-DIMENSIONAL FRACTIONAL-ORDER CHAOTIC SYSTEM BASED ON MULTIVARIATE MULTISCALE DISPERSION ENTROPY

1) MULTIVARIATE MULTISCALE DISPERSION ENTROPY ALGORITHM

In 2019, Azami *et al.* proposed multivariate multiscale dispersion entropy (mvMDE), which has the advantages such as fast calculation speed, good stability, and few storage elements [56]. The main calculation steps are as follows:

a: COARSE-GRAINED PROCESS OF MULTIPLE SIGNALS

It is assumed that a time series $U = \left\{u_{k,b}\right\}_{k=1,2,\cdots,p}^{b=1,2,\cdots,L}$ has p variables and its length is L. For each variable, the original signal is divided into non-overlapping segments of length τ. Then, the average value of each segment is calculated to derive the coarse-grained signal:

$$x_{k,i}^{(\tau)} = \frac{1}{\tau}\sum_{b=(i-1)\tau+1}^{i\tau} u_{k,b},\ 1 \le i \le \left\lfloor \frac{L}{\tau} \right\rfloor = N,\ 1 \le k \le p \tag{26}$$

where N represents the length of the coarse-grained signal.

b: CALCULATE MULTIVARIATE MULTISCALE DISPERSION ENTROPY

The steps are as follows:

(1) The multivariate signal $X = \left\{x_{k,i}\right\}_{k=1,2,\cdots,p}^{i=1,2,\cdots,N}$ is mapped into [1, 2,..., c].

(2) In order to consider the space domain and time domain at the same time, a multivariate embedding vector is created based on the Takens embedding theorem $Z_m(j),\ 1 \le j \le N-(m-1)d$. For simplicity, we assume that $d_k = d$, $m_k = m$.

(3) All combinations of $\sum_{k=1}^{p} m_k$ elements take once in $Z_m(j)$ and are called $\phi_q(j)(q = 1, \cdots, p)$. The number of combinations is equal to p. Therefore, there are $(N-(M-1)d)p$ dispersion modes for all variables.

(4) For the latent dispersion mode $\pi_{v_0\cdots v_{m-1}}$ corresponding to each c^m and $1 \le q \le p$, the relative frequency is as follows:

$$p(\pi_{v_0\cdots v_{m-1}}) = \frac{\#\left\{j \,|\, j \le N-(m-1)d, \phi_q(j)\ has\ type \pi_{v_0\cdots v_{m-1}}\right\}}{(N-(m-1)d)\,p} \tag{27}$$

(5) According to the definition of Shannon entropy, mvMDE can be expressed as:

$$mvMDE(X,m,c,d) = -\sum_{\pi=1}^{c^m} p(\pi_{v_0\cdots v_{m-1}}) \cdot \ln(p(\pi_{v_0\cdots v_{m-1}})) \tag{28}$$

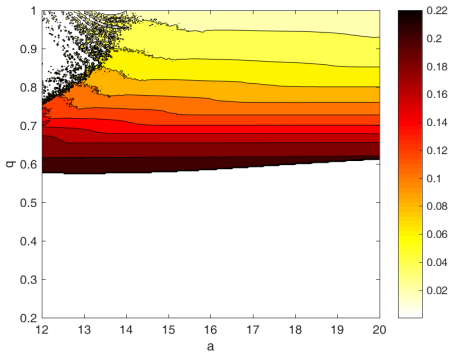

(a) Change trend of complexity with parameters a and q

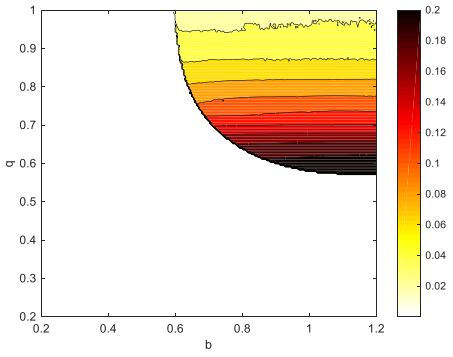

(b) Change trend of complexity with parameters b and q

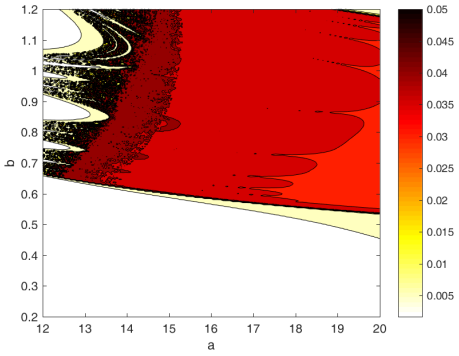

(c) Change trend of complexity with parameters a and b

FIGURE 9. mvMSE complexity chromatogram of fractional-order *a* chaotic system.

2) COMPLEXITY ANALYSIS OF THREE-DIMENSIONAL FRACTIONAL-ORDER CHAOTIC SYSTEM BASED ON MULTIVARIATE MULTISCALE DISPERSION ENTROPY

When order $q = 0.96$, system parameters $a \in (12, 20)$, $b = 1$, and $N = 15000$, the complexity of fractional-order a chaotic system is shown in Figure 11(a). When $a \in (12.14.13)$, the complexity oscillates violently and the complexity reaches the maximum when $a = 13.84$, and the complexity does not change and tends to be smooth until $a = 20$. When $a = 15$, $b = 1$, and $q \in (0.2, 1)$, the complexity of the fractional-order a chaotic system is shown in Figure 11(b). When $q \in (0.2, 0.5787)$, the complexity is in a slow growth trend. When $q = 0.584$, the complexity increases linearly and reaches the maximum, until the complexity decreases slowly when $q = 1$. When $a = 15$, $q = 0.96$, and $b \in (0.2, 1.2)$, the complexity of fractional-order a chaotic system is shown in Figure 11(c). When $b \in (0.2, 0.5967)$, the complexity increases slowly. When $b = 0.6$, the complexity increases sharply and reaches the maximum. Until $b = 1.2$, the complexity basically no longer changes and tends to be stable.

When $q = 0.96$, system parameters $a \in (14, 22)$, $b = 1, N = 15000$, the complexity of fractional-order b chaotic system is shown in Figure 12(a). When $a \in (14.14.59)$, the complexity decreases slowly with the increase of parameter a. When $a \in (14.13.15.87)$, the complexity increases greatly. When $a \in (15.87.17.41)$, the complexity basically oscillates. The maximum value of the complexity is reached when $a = 17.17$, and the complexity no longer changes significantly until $a = 22$. When $a = 18$, $b = 1$, and $q \in (0.2, 1)$, the complexity of fractional-order b chaotic system is shown in Figure 12(b). When $q \in (0.2.0.4053)$, the complexity increases slowly. Until $q = 0.4187$, the complexity increases sharply and reaches the maximum value, and until $q = 1$, the complexity decreases slowly. When $a = 18$, $q = 0.96$, and $b \in (0.2, 1.2)$, the complexity of fractional-order b chaotic system is shown in Figure 12(c). When $b \in (0.3533, 0.9333)$, the complexity is in an oscillating state. When $b = 0.6467$, the complexity reaches the regional maximum. It is also in a sharp oscillation trend until $b = 1.2$ and the oscillation frequency is faster than that when $b \in (0.3533, 0.9333)$.

For fractional-order a chaotic system, when $a \in (12, 20)$ and $q \in (0.2, 1)$, the chromatogram of complexity change is shown in Figure 13(a). When $q \in (0.576, 0.8827)$, the color is darker and the complexity is greater, and the complexity decreases as the order q increases. When $b \in (0.2, 1.2)$ and $q \in (0.2, 1)$, the chromatogram of complexity change is shown in Figure 13(b). The main complexity detection area is divided into the fan-shaped area and the left area. The complexity is maximum at the bottom of the fan-shaped region. Complexity decreases with the increase of order q

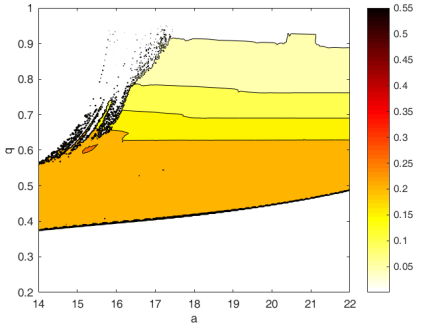

(a) Change trend of complexity with parameter a and q

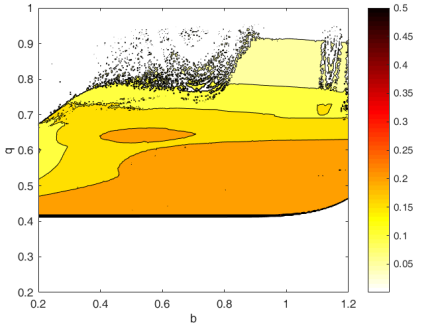

(b) Change trend of complexity with parameter b and q

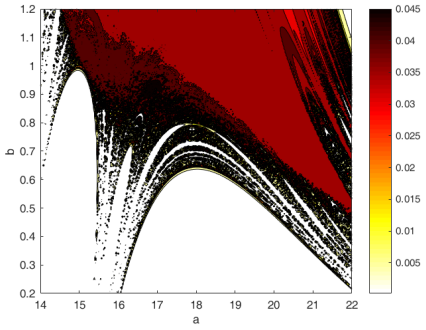

(c) Change trend of complexity with parameter a and b

FIGURE 10. mvMSE complexity chromatogram of fractional-order *b* chaotic system.

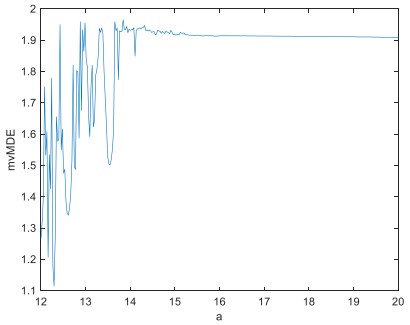

(a) Change trend of complexity with parameter a

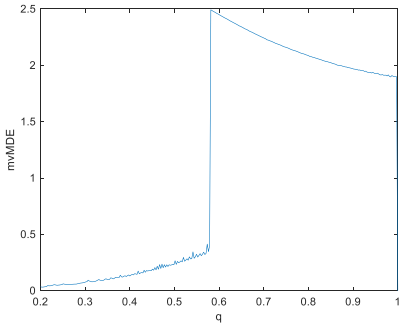

(b) Change trend of complexity with order q

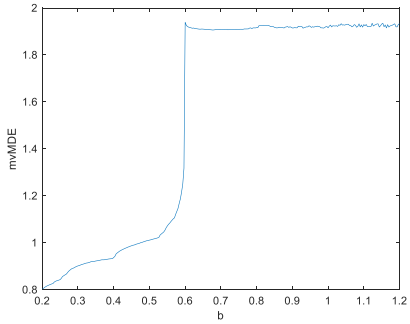

(c) Change trend of complexity with parameter b

FIGURE 11. Change trend of mvMDE complexity of fractional-order *a* chaotic system under single parameter.

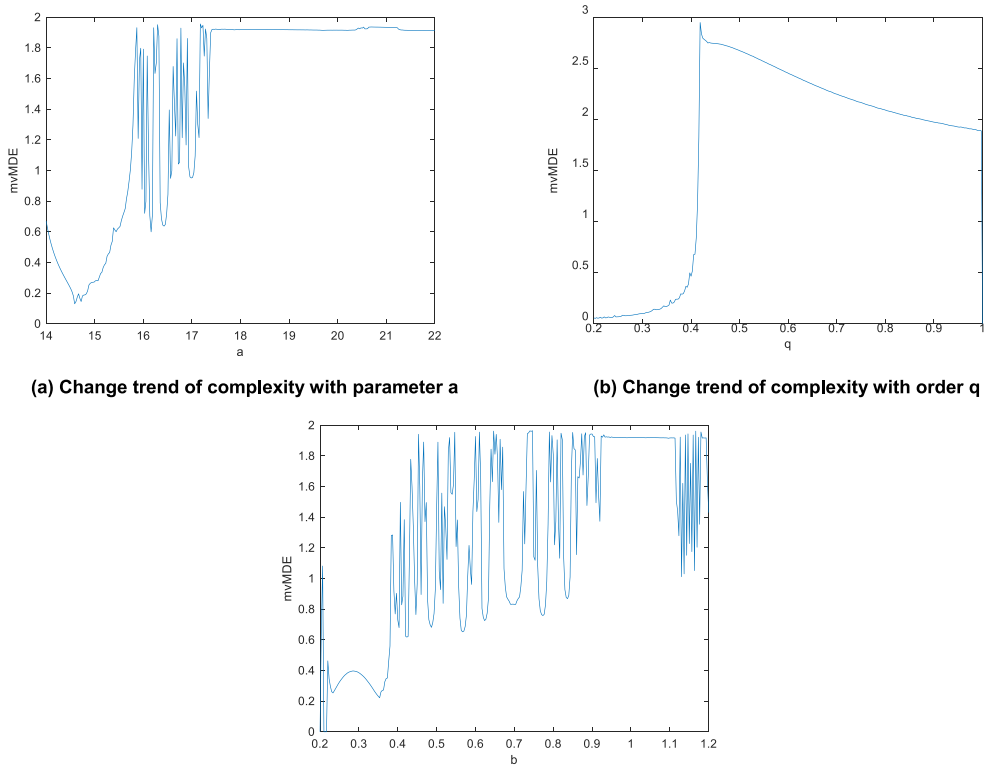

(a) Change trend of complexity with parameter a

(b) Change trend of complexity with order q

(c) Change trend of complexity with parameter b

FIGURE 12. Change trend of mvMDE complexity of fractional-order *b* chaotic system under single parameter.

in the fan-shaped region, and complexity increases with the increase of order q in the left area. When $a \in (12, 20)$, $b \in (0.2, 1.2)$, the chromatogram of complexity change is shown in Figure 13(c). When $q \in (0.53, 1)$, the color is the darkest, that is, the complexity is the largest. In the bottom area, the complexity also increases with the increase of the order q.

For fractional-order b system, when $a \in (14, 22)$ and $q \in (0.2, 1)$, the complexity change chromatogram is shown in Figure 14(a). It is easy to observe that the complexity of the upper left edge region is greater, and the overall complexity decreases as the order q increases. When $b \in (0.2, 1.2)$ and $q \in (0.2, 1)$, the complexity change chromatogram is shown in Figure 14(b), which is similar to Figure 14(a). The maximum complexity is mainly concentrated at the edge of the region and generally decreases with the increase of order q. When $a \in (14, 22)$ and $b \in (0.2, 1.2)$, the complexity change chromatogram is shown in Figure 14(c). It can be seen that the color in the right area is the darkest, that is, the complexity is the largest, while the complexity on the left is small.

D. PERFORMANCE COMPARISON OF DIFFERENT COMPLEXITY

This paper focuses on the performance of different algorithm when analyzing the complexity of three-dimensional fractional-order chaotic system. In the case of a single parameter, the maximum complexity that can be detected by different algorithm is shown in Table 1 and Table 2. In the case of two parameters, the maximum complexity that can be detected by different algorithm is shown in Table 3 and Table 4.

TABLE 1. Maximum complexity of single parameter in different algorithm of fractional-order *a* chaotic system.

	mvMFE	mvMSE	mvMDE
a	0.02138	0.05018	1.965
b	0.01989	0.04479	1.94
q	0.1066	0.2111	2.492

TABLE 2. Maximum complexity of single parameter in different algorithm of fractional-order *b* chaotic system.

	mvMFE	mvMSE	mvMDE
a	0.021	0.04843	1.956
b	0.02086	0.04888	1.964
q	0.2322	0.4449	2.949

Table 1 shows that for fractional-order a chaotic system, in the case of fixed system parameter b and order q, fixed system parameter a and order q, fixed system parameter a and b, the detection complexity by mvMFE is the lowest, and the detection complexity by mvMDE is the highest. Table 2 shows that for fractional-order b chaotic system,

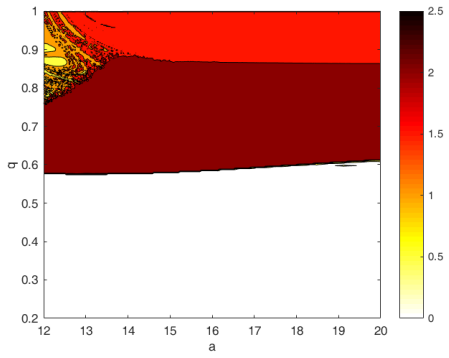

(a) Change trend of complexity with parameter a and q

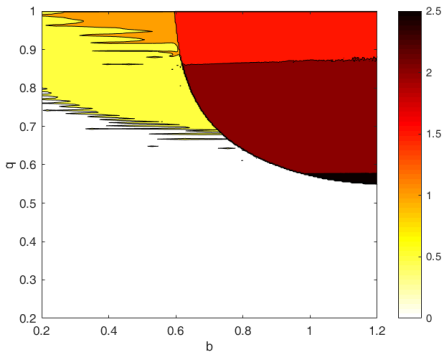

(b) Change trend of complexity with parameter b and q

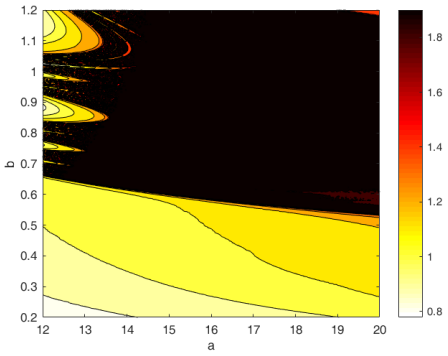

(c) Change trend of complexity with parameter a and b

FIGURE 13. mvMDE complexity chromatogram of fractional-order *a* chaotic system.

TABLE 3. Maximum complexity of two parameters in different algorithm of fractional-order *a* chaotic system.

	mvMFE	mvMSE	mvMDE
a、q	0.1	0.22	2.5
b、q	0.12	0.2	2.5
a、b	0.02	0.05	1.962

TABLE 4. Maximum complexity of two parameters in different algorithm of fractional-order *b* chaotic system.

	mvMFE	mvMSE	mvMDE
a、q	0.25	0.55	3
b、q	0.2	0.5	3
a、b	0.02	0.045	1.8

in the case of fixed system parameter b and order q, fixed system parameter a and order q, fixed system parameter a and b, the detection complexity by mvMFE is the lowest, and the detection complexity by mvMDE is the highest. Table 3 shows that for fractional-order a chaotic system, in the case of fixed system parameter b, fixed system parameter a, fixed order q, the detection complexity by mvMFE is the lowest, and the detection complexity by mvMDE is the highest. Table 4 shows that for fractional-order b chaotic system, in the case of fixed system parameter b, fixed system parameter a, fixed order q, the detection complexity by mvMFE is the lowest, and the detection complexity by mvMDE is the highest. From Figure 5, Figure 6, Figure 9, Figure 10, Figure 13 and Figure 14, it can be seen that in terms of the detection complexity range, the detection area of mvMFE is relatively small and the detection area of mvMDE is relatively large. The calculation speed of mvMFE is the slowest, and the calculation speed of mvMDE is the fastest. In summary, in terms of analyzing the complexity of three-dimensional fractional-order chaotic system, after analysis and comparison, the performance of mvMDE can be found to be the best.

In order to compare the influence of nonlinear term on the complexity, when the system parameters a and b are fixed, the complexity of fractional-order chaotic system is shown in Table 5. Since the mathematical models of the two selected fractional-order chaotic systems are basically similar, the difference is that in the z-plane expression, the fractional-order a chaotic system is a linear term and the fractional-order b chaotic system is a nonlinear term, so there is a good comparison. It can be seen from Table 5 that the fractional-order b chaotic system with one more nonlinear term is compared with the fractional-order a chaotic system, and the maximum complexity of the fractional-order b chaotic system is greater than that of the fractional-order a chaotic system. This shows that the nonlinearity in the mathematical model of fractional-order chaotic system is positively correlated with the change

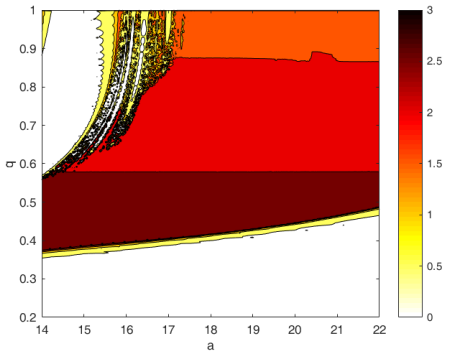

(a) Change trend of complexity with parameter a and q

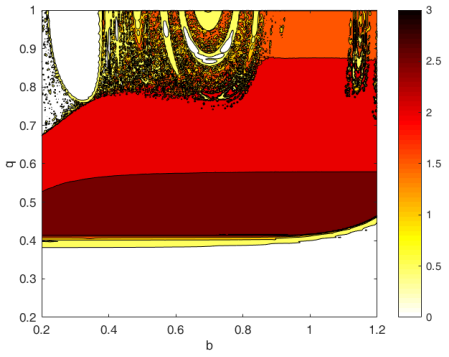

(b) Change trend of complexity with parameter b and q

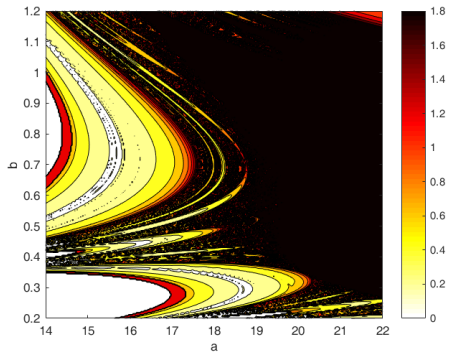

(c) Change trend of complexity with parameter a and b

FIGURE 14. mvMDE complexity chromatogram of fractional-order *b* chaotic system.

TABLE 5. The complexity of different system with varying order.

	mvMFE	mvMSE	mvMDE
fractional-order *a* chaotic system	0.1066	0.2111	2.492
fractional-order *b* chaotic system	0.2322	0.4449	2.949

in complexity. The fractional-order chaotic system with nonlinear term is more complex than the fractional-order chaotic system without nonlinear term, and the system itself is more chaotic.

V. DISCUSSION AND CONCLUSION

To solve the complexity problem of three-dimensional fractional-order chaotic system, this paper proposes complexity analysis of three-dimensional fractional-order chaotic system based on entropy theory. The discussion and conclusions are expanded as below.

(1) Complexity analysis of three-dimensional fractional-order chaotic system based on mvMFE, mvMSE, and mvMDE respectively is proposed.

(2) In the case of single parameter change, different entropy such as mvMFE, mvMSE, and mvMDE are used to analyze how complexity varies with parameter. Table 1 and Table 2 show that the detection complexity by mvMDE is the highest.

(3) In the case of two parameters change, the change of complexity is analyzed by the chromatomap which takes two parameters as independent variable, and mvMFE, mvMSE, and mvMDE as the dependent variable when the two parameters change simultaneously. Table 3 and Table 4 show that the detection complexity by mvMDE is the highest.

(4) Aiming at the performance problem, when the complexity of three-dimensional fractional-order chaotic system is analyzed by mvMFE, mvMSE, and mvMDE, the maximum complexity under single parameter and the detection area under two parameters are used as indicators. Then it is concluded that the performance of mvMDE is the best. It provides a new method for measuring the complexity of fractional-order chaotic system.

(5) In order to compare the influence of nonlinear term on the complexity, the mathematical models of the two selected fractional-order chaotic systems are basically similar. The difference is that in the z-plane expression, the fractional-order a chaotic system is a linear term and the fractional-order b chaotic system is a nonlinear term, so there is a good comparison. It can be seen from Table 5 that the maximum complexity of the fractional-order b chaotic system is greater than that of the fractional-order a chaotic system. This shows that the fractional-order chaotic system

with nonlinear term is more complex than the fractional-order chaotic system without nonlinear term, and the system itself is the more chaotic. This will lay the basis of theoretical analysis and practical application of fractional chaotic system in the fields of image encryption, sound encryption, image compression-encryption technique, and secure communication.

REFERENCES

[1] M. Wang, X. Liao, Y. Deng, Z. Li, Y. Su, and Y. Zeng, "Dynamics, synchronization and circuit implementation of a simple fractional-order chaotic system with hidden attractors," *Chaos, Solitons Fractals*, vol. 130, pp. 109406-1–109406-14, Jan. 2020.

[2] D. Baleanu and R. P. Agarwal, "Fractional calculus in the sky," *Adv. Difference Equ.*, vol. 2021, no. 1, pp. 117-1–117-9, Dec. 2021.

[3] H. Shao-Bo, S. Ke-Hui, and W. Hui-Hai, "Solution of the fractional-order chaotic system based on Adomian decomposition algorithm and its complexity analysis," *Acta Phys. Sinica*, vol. 63, no. 3, pp. 030502-1–030502-8, 2014.

[4] H. Chen, T. Lei, S. Lu, W. Dai, L. Qiu, and L. Zhong, "Dynamics and complexity analysis of fractional-order chaotic systems with line equilibrium based on Adomian decomposition," *Complexity*, vol. 2020, pp. 5710765-1–5710765-13, Oct. 2020.

[5] I. A. Mirza, M. S. Akram, N. A. Shah, S. Akhtar, and M. Muneer, "Study of one-dimensional contaminant transport in soils using fractional calculus," *Math. Methods Appl. Sci.*, vol. 44, no. 8, pp. 6839–6856, May 2021, doi: 10.1002/mma.7225.

[6] S. Rashid, Y. M. Chu, and J. Singh, "A unifying computational framework for novel estimates involving discrete fractional calculus approaches," *Alexandria Eng. J.*, vol. 60, pp. 893-1–893-22, Apr. 2020.

[7] M. P. Velasco, D. Usero, S. Jiménez, L. Vázquez, J. L. Vázquez-Poletti, and M. Mortazavi, "About some possible implementations of the fractional calculus," *Mathematics*, vol. 8, no. 6, pp. 21-1–21-9, 2015.

[8] C. G. Ma, M. Jun, Y. Cao, T. Liu, and J. Wang, "Multistability analysis of a conformable fractional-order chaotic system," *Phys. Scripta*, vol. 95, no. 7, pp. 075204-1–075204-23, 2020.

[9] X. Ye and X. Wang, "Characteristic analysis of a simple fractional-order chaotic system with infinitely many coexisting attractors and its DSP implementation," *Phys. Scripta*, vol. 95, no. 7, pp. 075212-1–075212-9, Jul. 2020.

[10] M. S. Tavazoei, "Fractional order chaotic systems: History, achievements, applications, and future challenges," *Eur. Phys. J. Special Topics*, vol. 229, nos. 6–7, pp. 887–904, Mar. 2020.

[11] G. Li, X. Zhang, and H. Yang, "Complexity analysis and synchronization control of fractional-order jafari-sprott chaotic system," *IEEE Access*, vol. 8, pp. 53360–53373, 2020.

[12] F. Yang and X. Wang, "Dynamic characteristic of a new fractional-order chaotic system based on the hopfield neural network and its digital circuit implementation," *Phys. Scripta*, vol. 96, no. 3, pp. 035218-1–035218-14, Jan. 2021.

[13] L. Lin, Q. Wang, B. He, Y. Chen, X. Peng, and R. Mei, "Adaptive predefined-time synchronization of two different fractional-order chaotic systems with time-delay," *IEEE Access*, vol. 9, pp. 31908–31920, 2021.

[14] F. Yang, J. Mou, C. Ma, and Y. Cao, "Dynamic analysis of an improper fractional-order laser chaotic system and its image encryption application," *Opt. Lasers Eng.*, vol. 129, pp. 106031-1–106031-16, Jun. 2020.

[15] P. Muthukumar, P. Balasubramaniam, and K. Ratnavelu, "Synchronization and an application of a novel fractional order king cobra chaotic system," *Chaos, Interdiscipl. J. Nonlinear Sci.*, vol. 24, no. 3, pp. 033105-1–033105-10, Sep. 2014.

[16] A. J. A. El-Maksoud, A. A. A. El-Kader, B. G. Hassan, N. G. Rihan, M. F. Tolba, L. A. Said, A. G. Radwan, and M. F. Abu-Elyazeed, "FPGA implementation of sound encryption system based on fractional-order chaotic systems," *Microelectron. J.*, vol. 90, pp. 323–335, Aug. 2019.

[17] Y.-G. Yang, B.-W. Guan, Y.-H. Zhou, and W.-M. Shi, "Double image compression-encryption algorithm based on fractional order hyper chaotic system and DNA approach," *Multimedia Tools Appl.*, vol. 80, no. 1, pp. 691–710, Jan. 2021.

[18] Y.-G. Yang, B.-W. Guan, J. Li, D. Li, Y.-H. Zhou, and W.-M. Shi, "Image compression-encryption scheme based on fractional order hyper-chaotic systems combined with 2D compressed sensing and DNA encoding," *Opt. Laser Technol.*, vol. 119, pp. 105661-1–105661-14, Nov. 2019.

[19] M. Lahdir, H. Hamiche, S. Kassim, M. Tahanout, K. Kemih, and S.-A. Addouche, "A novel robust compression-encryption of images based on SPIHT coding and fractional-order discrete-time chaotic system," *Opt. Laser Technol.*, vol. 109, pp. 534–546, Jan. 2019.

[20] R.-G. Li and H.-N. Wu, "Secure communication on fractional-order chaotic systems via adaptive sliding mode control with teaching–learning–feedback-based optimization," *Nonlinear Dyn.*, vol. 95, no. 2, pp. 1221–1243, Jan. 2019.

[21] A. Soleimanizadeh and M. A. Nekoui, "Optimal type-2 fuzzy synchronization of two different fractional-order chaotic systems with variable orders with an application to secure communication," *Soft Comput.*, vol. 25, no. 8, pp. 6415–6426, Apr. 2021, doi: 10.1007/s00500-021-05636-1.

[22] J. J. Montesinos-García and R. Martínez-Guerra, "A numerical estimation of the fractional-order liouvillian systems and its application to secure communications," *Int. J. Syst. Sci.*, vol. 50, no. 4, pp. 791–806, Mar. 2019.

[23] S. He, K. Sun, and X. Wu, "Fractional symbolic network entropy analysis for the fractional-order chaotic systems," *Phys. Scripta*, vol. 95, no. 3, pp. 035220-1–035220-20, Mar. 2020.

[24] H. Rabarimanantsoa, L. Achour, C. Letellier, A. Cuvelier, and J.-F. Muir, "Recurrence plots and Shannon entropy for a dynamical analysis of asynchronisms in noninvasive mechanical ventilation," *Chaos, Interdiscipl. J. Nonlinear Sci.*, vol. 17, no. 1, pp. 013115-1–013115 -10, Mar. 2007.

[25] S. He, K. Sun, and R. Wang, "Fractional fuzzy entropy algorithm and the complexity analysis for nonlinear time series," *Eur. Phys. J. Special Topics*, vol. 227, nos. 7–9, pp. 943–957, Oct. 2018.

[26] S. He and S. Banerjee, "Epidemic outbreaks and its control using a fractional order model with seasonality and stochastic infection," *Phys. A, Stat. Mech. Appl.*, vol. 501, pp. 408–417, Jul. 2018.

[27] F. Yang, J. Mou, J. Liu, C. Ma, and H. Yan, "Characteristic analysis of the fractional-order hyperchaotic complex system and its image encryption application," *Signal Process.*, vol. 169, pp. 107373-1–107373-16, Apr. 2020.

[28] L. Cui, M. Lu, Q. Ou, H. Duan, and W. Luo, "Analysis and circuit implementation of fractional order multi-wing hidden attractors," *Chaos, Solitons Fractals*, vol. 138, pp. 109894-1–109894-12, Sep. 2020.

[29] B. Yan, S. He, K. Sun, and S. Wang, "Complexity and multistability in the centrifugal flywheel governor system with stochastic noise," *IEEE Access*, vol. 8, pp. 30092–30103, 2020.

[30] S. He, K. Sun, and H. Wang, "Multivariate permutation entropy and its application for complexity analysis of chaotic systems," *Phys. A, Stat. Mech. Appl.*, vol. 461, pp. 812–823, Nov. 2016.

[31] L. Wang, K. Sun, Y. Peng, and S. He, "Chaos and complexity in a fractional-order higher-dimensional multicavity chaotic map," *Chaos, Solitons Fractals*, vol. 131, pp. 109488-1–109488-10, Feb. 2020.

[32] A. Ouannas, A. A. Khennaoui, S. Momani, V.-T. Pham, and R. El-Khazali, "Hidden attractors in a new fractional–order discrete system: Chaos, complexity, entropy, and control," *Chin. Phys. B*, vol. 29, no. 5, pp. 050504-1–050504-18, May 2020.

[33] A. A. Khennaoui, A. O. Almatroud, A. Ouannas, M. M. Al-Sawalha, G. Grassi, V.-T. Pham, and I. M. Batiha, "An unprecedented 2-dimensional discrete-time fractional-order system and its hidden chaotic attractors," *Math. Problems Eng.*, vol. 2021, pp. 6768215-1–6768215-10, Jan. 2021.

[34] A. Ouannas, A.-A. Khennaoui, S. Momani, G. Grassi, V.-T. Pham, R. El-Khazali, and D. V. Hoang, "A quadratic fractional map without equilibria: Bifurcation, 0–1 test, complexity, entropy, and control," *Electronics*, vol. 9, no. 5, pp. 748-1–748-15, May 2020.

[35] A. A. Khennaoui, A. Ouannas, S. Boulaaras, V.-T. Pham, and A. T. Azar, "A fractional map with hidden attractors: Chaos and control," *Eur. Phys. J. Special Topics*, vol. 229, nos. 6–7, pp. 1083–1093, Mar. 2020.

[36] J. Li, P. Shang, and X. Zhang, "Financial time series analysis based on fractional and multiscale permutation entropy," *Commun. Nonlinear Sci. Numer. Simul.*, vol. 78, pp. 104880-1–104880-13, Nov. 2019.

[37] Y. Liu, D. Wang, Y. Ren, and N. Jin, "Detecting the flow pattern transition in the gas-liquid two-phase flow using multivariate multi-scale entropy analysis," *Zeitschrift Naturforschung A*, vol. 74, no. 10, pp. 837–848, Sep. 2019.

[38] I. Petráš and J. Terpák, "Fractional calculus as a simple tool for modeling and analysis of long memory process in industry," *Mathematics*, vol. 7, no. 6, pp. 511-1–511-9, Jun. 2019.

[39] M. Matusiak, "Optimization for software implementation of fractional calculus numerical methods in an embedded system," *Entropy*, vol. 22, no. 5, pp. 566-1–566-14, May 2020.

[40] H. Fu, G.-C. Wu, G. Yang, and L.-L. Huang, "Fractional calculus with exponential memory," *Chaos*, vol. 31, no. 3, pp. 031103-1–031103-10, 2021.
[41] Y. Luchko, "Fractional derivatives and the fundamental theorem of fractional calculus," *Fractional Calculus Appl. Anal.*, vol. 23, no. 4, pp. 939–966, Aug. 2020.
[42] C. Yang, F. Xie, Y. Chen, W. Xiao, and B. Zhang, "Modeling and analysis of the fractional-order flyback converter in continuous conduction mode by caputo fractional calculus," *Electronics*, vol. 9, no. 9, pp. 1544-1–1544-14, Sep. 2020.
[43] E. C. de Oliveira, S. Jarosz, and J. Vaz, "Fractional calculus via Laplace transform and its application in relaxation processes," *Commun. Nonlinear Sci. Numer. Simul.*, vol. 69, pp. 58–72, Apr. 2019.
[44] X. Lü and G. T. Liu, "Comparison of several common fractional calculus definitions," *J. Inner Mongolia Normal Univ., Natural Sci. Ed.*, vol. 46, no. 4, pp. 479–482, 2017.
[45] L. X. Wei, H. Wang, and X. W. Mu, "Control of revolving inverted pendulum based on PSO-FOPID controller," *Control Eng. China*, vol. 26, no. 2, pp. 196–201, 2019.
[46] Z. Guang-Chao, L. Chong-Xin, and W. Yan, "Dynamic analysis and finite time synchronization of a fractional-order chaotic system with hidden attractors," *Acta Phys. Sinica*, vol. 67, no. 5, pp. 050502-1–050502-8, 2018.
[47] S. Jafari and J. C. Sprott, "Simple chaotic flows with a line equilibrium," *Chaos, Solitons Fractals*, vol. 57, pp. 79–84, Dec. 2013.
[48] H. Jia, Z. Guo, G. Qi, and Z. Chen, "Analysis of a four-wing fractional-order chaotic system via frequency-domain and time-domain approaches and circuit implementation for secure communication," *Optik*, vol. 155, pp. 233–241, Feb. 2018.
[49] A.-H. Tian, C.-B. Fu, X.-Y. Su, and H.-T. Yau, "Lathe tool chatter vibration diagnostic using general regression neural network based on Chua's circuit and fractional-order Lorenz master/slave chaotic system," *J. Low Freq. Noise, Vib. Act. Control*, vol. 38, nos. 3–4, pp. 953–966, Dec. 2019.
[50] L. Zhao and W. Deng, "Jacobian-predictor-corrector approach for fractional differential equations," *Adv. Comput. Math.*, vol. 40, no. 1, pp. 137–165, Feb. 2014.
[51] C. Zhang and J. Xiao, "Chaotic behavior and feedback control of magnetorheological suspension system with fractional-order derivative," *J. Comput. Nonlinear Dyn.*, vol. 13, no. 2, pp. 021007-1–021007-9, Feb. 2018.
[52] T. Liu, H. Yan, S. Banerjee, and J. Mou, "A fractional-order chaotic system with hidden attractor and self-excited attractor and its DSP implementation," *Chaos, Solitons Fractals*, vol. 145, pp. 110791-1–110791-12, Apr. 2021.
[53] B. Yan and S. B. He, "Dynamics and complexity analysis of the conformable fractional-order two-machine interconnected power system," *Math. Methods Appl. Sci.*, vol. 44, no. 3, pp. 2439–2454, 2019.
[54] M. Ahmed, T. Chanwimalueang, S. Thayyil, and D. Mandic, "A multivariate multiscale fuzzy entropy algorithm with application to uterine EMG complexity analysis," *Entropy*, vol. 19, no. 1, pp. 2-1–2-18, Dec. 2016.
[55] M. U. Ahmed and D. P. Mandic, "Multivariate multiscale entropy analysis," *IEEE Signal Process. Lett.*, vol. 19, no. 2, pp. 91–94, Feb. 2012.
[56] H. Azami, A. Fernández, and J. Escudero, "Multivariate multiscale dispersion entropy of biomedical times series," *Entropy*, vol. 21, no. 9, pp. 913-1–913-21, Sep. 2019.

GUOHUI LI received the bachelor's degree in electronic information engineering from the Chongqing University of Technology, Chongqing, China, in 2001, the master's degree in circuit and system degree from the University of Electronic Science and Technology of China, Chengdu, China, in 2004, and the doctor's degree in acoustics from Northwestern Polytechnical University, Xi'an, China, in 2015. He is currently an Associate Professor with the School of Electronic Engineering, Xi'an University of Posts & Telecommunications, Xi'an. His research interests include underwater acoustic signal processing, and chaotic signal processing.

XIANGYU ZHANG received the bachelor's degree in measurement and control technology and instruments from the Baoji College of Arts and Sciences, Baoji, China, in 2018. He is currently pursuing the master's degree in electronics and communication engineering with the Xi'an University of Posts & Telecommunications, Xi'an, China. His research interests include characteristics of fractional-order chaotic systems, and synchronization control.

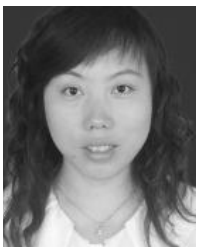

HONG YANG received the bachelor's and master's degrees in mechanical and electronic engineering from the University of Electronic Science and Technology of China, Chengdu, China, in 2003 and 2006, respectively, and the doctor's degree in acoustics from Northwestern Polytechnical University, Xi'an, China, in 2015. She is currently an Associate Professor with the School of Electronic Engineering, Xi'an University of Posts & Telecommunications, Xi'an. Her research interests include underwater acoustic signal processing, and chaotic signal processing.